

Solar Reforming of Biomass with Homogeneous Carbon Dots

Demetra S. Achilleos,^[a] Wenxing Yang,^[b] Hatice Kasap,^[a] Aleksandr Savateev,^[c] Yevheniia Markushyna,^[c] James R. Durrant,^{*[b]} and Erwin Reisner^{*[a]}

[a] Dr. D. S. Achilleos, Dr. H. Kasap, Prof. E. Reisner
Christian Doppler Laboratory for Sustainable SynGas Chemistry, Department of Chemistry, University of Cambridge, Lensfield Road, Cambridge CB2 1EW, UK; E-mail: reisner@ch.cam.ac.uk

[b] Dr. W. Yang, Prof. J. R. Durrant
Department of Chemistry, Imperial College London, Exhibition Road, London SW7 2AZ, UK. E-mail: j.durrant@imperial.ac.uk

[c] Dr. A. Savateev, Y. Markushyna
Department of Colloid Chemistry, Max-Planck Institute of Colloids and Interfaces, Research Campus Golm, 14424 Potsdam, Germany

Supporting information for this article is given via a link at the end of the document.

Abstract: A sunlight-powered process is reported that employs carbon dots (CDs) as light absorber for the conversion of lignocellulose into sustainable H₂ fuel and organics. This photocatalytic system operates in pure and untreated sea water using a benign pH (2-8) at ambient temperature and pressure. The CDs can be produced in a scalable synthesis directly from biomass itself and their solubility allows for good interactions with the insoluble biomass substrates. They also display excellent photophysical properties with a reductive and an oxidative quenching pathway. The presented CD-based biomass photoconversion system opens new avenues for sustainable, practical, and renewable fuel production through biomass valorization.

Photocatalysis allows for the utilization of solar energy to produce renewable H₂, but most reported systems still require precious-metal components, purified water or an expensive sacrificial electron donor (ED).^[1] Photoreforming (PR) can use sunlight to convert biomass waste into H₂ and organic chemicals.^[2] Instead of oxidizing water as in classical artificial photosynthesis,^[3] PR employs preferentially abundant and inedible lignocellulose as an ED to quench holes (h⁺) in a photoexcited photocatalyst, leaving behind low-potential electrons to drive proton reduction.^[4] PR commonly relies on UV-absorbing TiO₂ colloids with noble metal cocatalysts (Pt, RuO₂),^[5] and toxic CdS in organic solvents (CH₃CN)^[6] or alkaline conditions (pH > 14).^[7] Carbon nitride (CN_x) has been shown for visible-light driven PR of biomass under benign aqueous pH,^[8] but the heterogeneous nature of CN_x restricts effective substrate/photocatalyst interactions to occur.^[2b] Previous PR systems have also shown conversion yields ≤ 22% (under strongly alkaline conditions) and required purified water,^[5-8] which limit their utility, sustainability and economics.

Here, we introduce homogeneous carbon dots (CDs, **Figure 1**) produced from controlled, scalable calcination of cellulose (α -*cel*-CDs at 320 °C, **Figure S1**),^[9] or commercial precursors such as citric acid (resulting in amorphous CDs, *a*-CDs at 180, and *g*-CDs at 320 °C),^[10] and aspartic acid (resulting in graphitic N-doped CDs at 320 °C, *g*-N-CDs; see S1)^[10b, 11] for biomass PR. The non-toxic, biocompatible CDs are employed as light absorbers, together with a Ni bis(diphosphine) H₂ evolution cocatalyst (**NiP**,^[12] **Figure S2**), to produce H₂ and organics in purified and untreated water (**Figure 1b**) under benign conditions. Transient absorption spectroscopy provides insight into the electron transfer dynamics of the PR systems.

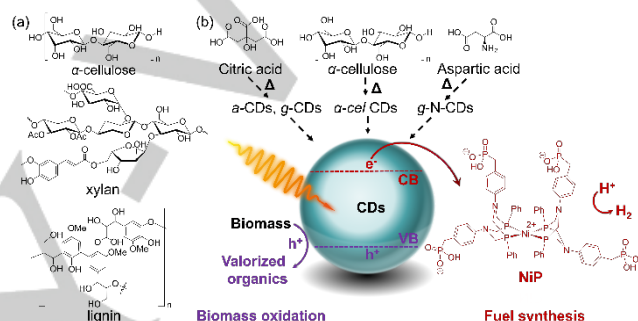


Figure 1. (a) Chemical structures of lignocellulosic components used as EDs. (b) CDs are synthesized from biomass (α -cellulose) or commercial precursors (citric, aspartic acid) and used with **NiP** as cocatalyst in PR of biomass to coproduce H₂ and oxidized organics.

α -*cel*-CDs (diameter: 9 \pm 3 nm) and *g*-N-CDs (3 \pm 1 nm) are graphitic with (100) intralayer spacings of 3.0 and 2.4 Å, respectively.^[9, 10b] Powder XRD also suggests nanocrystalline, low defect graphitic structures for α -*cel*-CDs (27.6° 2 θ) and *g*-N-CDs (27.0° 2 θ), in agreement with Raman (graphitic content, G band, 1570-1580 cm⁻¹ and defects, D band, 1331-1340 cm⁻¹) and ¹³C NMR spectroscopy (predominant sp² environments, δ = 110-180 ppm, no sp³ centers).^[9, 10b] *g*-CDs (4 \pm 1 nm) are graphitic, whereas *a*-CDs (7 \pm 2 nm) are amorphous.^[10]

Photocatalysis with the CDs (0.03–2.8 mg) and **NiP** (50 nmol) was first performed using ethylenediaminetetraacetic acid (EDTA, 0.1 M, pH 6) as the sacrificial ED in purified water (3 mL; **Figure 2a, S3**). All systems were irradiated with simulated solar light (AM 1.5G, 100 mW cm⁻²) under an inert atmosphere at 25 °C and the headspace gas was analyzed by gas chromatography. H₂ yields (in μ mol, **Figure 2a**) and specific activities (μ mol H₂ (g_{CDs})⁻¹ h⁻¹, **Figure S3, Tables S1-S4**) were optimized by varying the amounts of CDs. α -*cel*-CDs showed consistently the highest H₂ yields with their best performance at 2.2 mg (15.6 \pm 0.7 μ mol H₂, 24 h, **Figure 2a**). The α -*cel*-CDs/**NiP** system was also photocatalytically active under visible-light only irradiation (λ > 400 nm, **NiP**), albeit with a lower H₂ yield (28%). CDs have sufficient driving force for proton reduction (CB at approximately -0.5 V vs. RHE)^[13], however, the accurate determination of their band levels is crucial for their future development as photocatalysts.

The α -*cel*-CD/**NiP** system provides a benchmark activity of $13,450 \mu\text{mol H}_2 (\text{g}_{\text{CDs}})^{-1} \text{h}^{-1}$ (Figure S3), which is the highest reported so far for carbonaceous photoabsorbers using comparable conditions (Table S5).^[10-11, 14] The α -*cel*-CDs display a maximum internal quantum efficiency (IQE at $\lambda = 360 \text{ nm}$, $I = 4.05 \text{ mW cm}^{-2}$) of 11.4%, which compares favorably with *g*-N-CDs (5.3%) and *a*-CDs (1.4 %).^[10b] Future improvements in the development of the CDs should focus on high IQEs in the visible region. The photo-stability of the CD/**NiP** systems is currently limited by the fragile ligand framework of **NiP**, which degrades after a few hours of operation due to formation of radicals from EDTA oxidation or ligand displacement from the Ni center.^[13] 4-methylbenzyl alcohol (30 μmol) instead of EDTA produced $3.7 \pm 0.2 \mu\text{mol H}_2$ after 6 h irradiation with α -*cel*-CD/**NiP** (Figure S4, Table S6).

We then studied various insoluble biomass (α -cellulose, xylan and lignin; Figure 1a) and soluble biomass model substrates and alcohols of industrial relevance (ethanol, glycerol; Figure S5). PR in aqueous phosphate solution (KP_i ; pH 6 and 25 °C) with the CDs showed activity under benign conditions (Figures 2b, S6; Tables S6-S9), with the α -*cel*-CDs showing again the best activity (Figures 2b).

The highest H_2 yields after 24 h were observed with galactose ($8.8 \pm 0.2 \mu\text{mol}$) and glycerol ($8.5 \pm 0.1 \mu\text{mol}$), which correspond to turnover numbers of **NiP** (TON_{NiP}) of 177 ± 4 and 170 ± 2 , respectively. Control experiments without ED, CDs or **NiP** showed negligible or no H_2 evolution (Figure S7 and Table S7). The lowest H_2 yields were observed for lignin ($0.03 \mu\text{mol}$) due to its strong light absorption and robust cross-linked polyphenolic structure.^[15] However, a much higher H_2 yield ($7.8 \pm 0.5 \mu\text{mol}$, Table S6) was observed at lower lignin quantities (0.5 mg) due to improved light penetration through the CD solution (Figure 2b, empty bar). PR of α -cellulose and xylan produced 5.0 ± 0.2 and $3.6 \pm 0.3 \mu\text{mol H}_2$, respectively, similar to a heterogeneous CN_x/NiP system.^[8a] However, in contrast to heterogeneous systems that show substrate-dependent H_2 yields, homogeneous CDs photoreform soluble and insoluble biomass with a similar efficiency.

PR of α -cellulose with the α -*cel*-CD/**NiP** system was subsequently studied in KP_i (pH 4.5, 6 and 8), H_2SO_4 (pH 2) and 10 M KOH (\sim pH 15) (Figure S8). The highest H_2 yields after 24 h were observed at pH 6 ($5.0 \pm 0.2 \mu\text{mol H}_2$) and pH 8 ($3.6 \pm 0.2 \mu\text{mol H}_2$). The efficiency was decreased approximately four times ($1.2 \pm 0.1 \mu\text{mol H}_2$) in strong acid (pH 2), and PR did not proceed under extremely basic conditions (10 M KOH) due to chemical instability of **NiP** (Figure S8 and Table S10).^[13]

The biomass conversion yield (CY, %) was determined in KP_i pH 6 with α -*cel*-CD/**NiP** at various α -cellulose loadings (0.8–1.65 mg, Figure S9, Table S11). A CY of 13.4% was achieved at 0.8 mg α -cellulose (12 hrs), whereas re-additions of **NiP** (50 nmol) to repair the PR system *in situ* allowed a CY of 34.1% (48 h, Figure S9).^[13] This is higher than CYs reported for CdS/CdO_x (9.7%)^[7] and CN_x/Pt (22%)^[8a] under strongly alkaline conditions.

The oxidation products were determined by High Performance Liquid Chromatography Mass Spectrometry (HPLC/MS) and ^1H , ^{13}C NMR spectroscopy after PR of α -cellulose, xylan, glucose and galactose with α -*cel*-CDs (2.2 mg) and **NiP** (50 nmol) in KP_i (pH 6; see Figures S10-S17 for detailed analysis). In brief, the main products of α -cellulose PR are $\text{C}_6\text{H}_{12}\text{O}_6$ and $\text{C}_6\text{H}_{10}\text{O}_5$ compounds (e.g., 2,5-anhydro-D-mannofuranose isomers). HPLC/MS and ^{13}C NMR spectroscopy

suggest the formation of 2,3,4,5,6-pentahydroxyhexanoate along with other oligosaccharides after PR of uniformly ^{13}C -labeled cellulose. PR of xylan produced hydroferulic acid $\text{C}_{10}\text{H}_{12}\text{O}_4/\text{C}_{11}\text{H}_{14}\text{O}_4$ derivatives and other depolymerization products. PR of galactose/glucose resulted in $\text{C}_6\text{H}_{12}\text{O}_6$ and $\text{C}_6\text{H}_{10}\text{O}_5$ isomers.

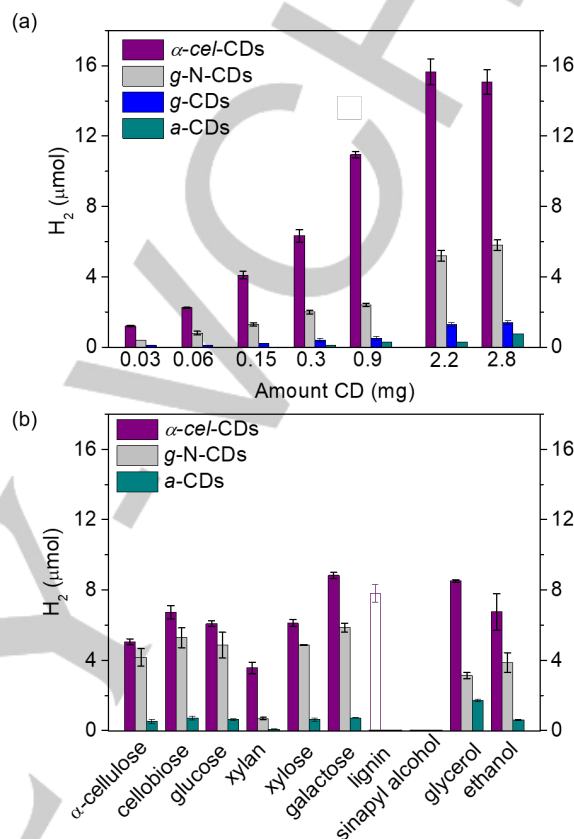


Figure 2. (a) Photo- H_2 evolution using α -*cel*-CDs, *g*-N-CDs, *g*-CDs and *a*-CDs (0.03–2.8 mg) and EDTA (0.1 M, pH 6, 3 mL) as sacrificial ED. (b) Photo- H_2 evolution with α -*cel*-CDs (2.2 mg), *g*-N-CDs (0.5 mg) and *a*-CDs (10 mg) using pure lignocellulosic components and soluble substrates (100 mg, solid bars) in purified water (KP_i , pH 6). The empty bar shows the result using 0.5 mg of lignin. Conditions: AM 1.5G (100 mW cm^{-2}) irradiation, with **NiP** (50 nmol) for 24 h and 25 °C.

PR of α -*cel*-CDs (2.2 mg) with biomass substrates (100 mg) was then studied in untreated sea water (adjusted pH = 6; Figures S18-S19, Tables S12-S14). The H_2 yields are comparable to purified water as reaction medium, suggesting that impurities/background organics do not hinder photocatalysis as observed for TiO_2 -based systems, but rather act as EDs.^[16] The highest H_2 yields were again achieved with galactose ($8.4 \pm 0.1 \mu\text{mol}$, 24 h). The *g*-N-CDs showed 2–7 times lower H_2 yields in sea water compared to purified water ($\leq 2.3 \pm 0.1 \mu\text{mol}$, 24 h), presumably due to N-doping which may provide adsorption sites for contaminants from the impurity-rich water.^[16a] *a*-CDs in sea water show low H_2 yields ($\leq 0.3 \mu\text{mol}$), comparable to purified water. Thus, undoped CDs maintain good photocatalytic performances under real-world conditions.^[16a]

TA spectroscopy was employed to study the photophysics and charge transfer properties of α -*cel*-CDs, on fs–ns (fs-TA) or μs –s (μs -TA) timescales. fs-TA spectra (355 nm excitation, under

COMMUNICATION

Ar) resulted in a broad absorption feature in the visible region (Figure S20), which decays ~2 fold faster upon adding EDTA, with the decay half-life changing from ~20 to 40 ps (Figure 3a). This indicates that the absorption contains a partial contribution from photoinduced h^+ that are scavenged by EDTA (~0.1 ns),^[8c, 16c] most likely by pre-adsorbed ED species.

On μ s–s timescales, a blue-shifted, long-lived signal is observed in the absence of EDTA (Figure S21), which is effectively quenched by O_2 and thus originates primarily from electrons. These are long-lived, trapped charge carriers with residual signals (~100 ms) even without EDTA, similar to previous reports for C_3N_4 ,^[17] and metal oxide photocatalysts.^[18] Addition of NiP as electron scavenger for α -cel-CDs resulted in (i) quenching of the electron signal (~0.5 ms) and (ii) appearance of a negative signal, assigned to the ground-state bleach of NiP due to its reduction by CDs, at 500 nm (Figures 3b, S22).^[10b, 12, 19] This suggests the direct electron transfer from CDs to NiP, even without EDTA, therefore demonstrating an oxidative quenching mechanism. Titration of CDs with NiP (Figure S23) revealed a linear relationship between the electron decay rates (at 500 nm) and NiP concentration, and an oxidative quenching rate of $1.09 \pm 0.04 \times 10^8 \text{ M}^{-1} \text{ s}^{-1}$. This mechanism will have a low overall yield, as without EDTA most electrons recombine on faster timescales ($\ll 100$ ms), consistent with negligible H_2 production (Table S7). Nevertheless, the ability of long-lived trapped electrons to reduce NiP indicates that they retain reactivity, with trap energies above the NiP reduction potential.

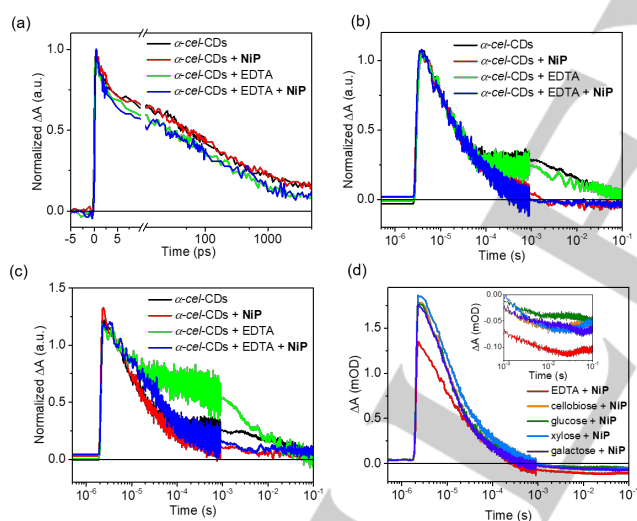


Figure 3. Normalized (a) (~1 ps) fs-TA kinetics between 500 and 520 nm, (b) (~50 μ s) μ s-TA kinetics (electrons) at 500 nm, (c) (~50 μ s) μ s-TA kinetics (electrons) at 700 nm of α -cel-CDs with EDTA and/or NiP. (d) Normalized (~50 μ s) μ s-TA kinetics (electrons) of α -cel-CDs at 500 nm with NiP and various biomass EDs (0.1 M). Inset shows the bleach region of ΔA which corresponds to NiP⁻. Conditions: KP_i (pH = 6.6) with NiP (50 nmol) upon excitation at 355 nm with an energy of 1 mJ cm^{-2} .

Consistent with the fast hole scavenging process (~0.1 ns), addition of EDTA resulted in prolonged electron signals at 700 nm (Figure 3c), indicative of reductive quenching. Signals at 500 nm were not prolonged with EDTA, suggesting multiple electronic states in the α -cel-CDs.^[20] Nevertheless, these results show both oxidative and reductive quenching for α -cel-CDs, which is different from that observed for g -N-CDs and a -CDs under similar

conditions. In the latter cases, NiP⁻ can only be formed with EDTA,^[10b] most likely due to differences in energy of the trapped charges between these samples. For α -cel-CDs, the appearance of the NiP⁻ signal at 500 nm at long times (Figures S22e) is indicative of reasonably efficient photoinduced NiP reduction (Figure 4).

Previous studies on g -N-CDs showed a bimolecular recombination lifetime of $t_{50\%} = 9$ ps, with a residual 6% of long-lived carriers (5 ns) to drive H_2 production.^[10b] Herein, using similar excitation fluence/buffer conditions, the α -cel-CD bimolecular recombination lifetime is $t_{50\%} = 45 \pm 5$ ps (*i.e.*, 5 times slower), with the proportion of long-lived (> 5 ns) carriers being about 15–20% (Figure 3a). We can thus propose two reasons for improved photocatalysis with α -cel-CDs: (i) existence of both oxidative and reductive quenching mechanisms and (ii) α -cel-CDs show slower bimolecular recombination processes and higher yields of long-lived carriers, which enable higher H_2 yields both under model (Figure 2a) and real-world conditions (Figure S18).

Finally, μ s-TA spectra of α -cel-CDs with biomass were collected to analyze their capacity to quench the photogenerated h^+ . Biomass addition induced a similar oxidative quenching mechanism as with EDTA (Figures S24), but with a 50% lower yield of NiP⁻ (Figure 3d). The slower h^+ extraction is assigned to the less accessible biomass compared to EDTA, which results in increased recombination and thus fewer long-lived electrons that to be extracted by NiP. This agrees with photocatalysis, where twice the H_2 yield was observed with EDTA compared to biomass (Figure 2). It is also possible that long-lived, trapped h^+ accumulate in CDs with biomass as ED due to the oxidative quenching pathway by NiP (Figure 4, white panel), facilitating oxidation of the challenging lignocellulosic substrates.

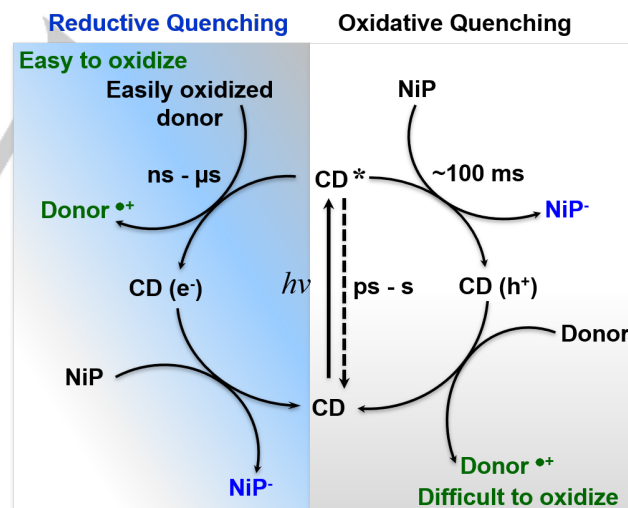


Figure 4. Timescales of relaxation and possible charge transfer reactions under photocatalytic conditions for α -cel-CDs.

In summary, we report the development of a homogeneous PR system using CDs as light absorbers, which use the nexus of natural resources for coupled sustainable fuel production with biomass utilization and chemical synthesis. CDs prepared from biomass have well-suited photophysical characteristics such as the availability of an oxidative quenching pathway to convert challenging substrates and a high fraction of long-lived charge

carriers. The cellulose-derived CDs allow solar-driven fuel synthesis from lignocellulosic biomass under benign conditions with the prospect to simultaneously produce valuable chemicals in solution. Such systems, which use a noble metal-free cocatalyst, maintain their photocatalytic activity even in untreated sea water, which creates promising perspectives for the development of energy self-sufficient and low-carbon economies.

Acknowledgements

This work was financially supported by the Christian Doppler Research Association (Austrian Federal Ministry for Digital and Economic Affairs and the National Foundation for Research, Technology and Development) and OMV. W.Y. acknowledges support from the Swedish Research Council for an International Postdoc Fellowship.

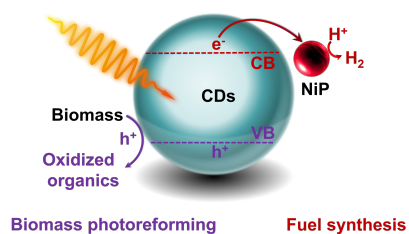
Conflict of Interest

A patent application on the reported work has been filed by Cambridge Enterprise (international patent number: WO 2019/229255) which lists D.S.A., H.K. and E.R. as the inventors.

Keywords: biomass • photoreforming • carbon dots • hydrogen • organics

- [1] a) Y. Pellegrin, F. Odobel, *C. R. Chim.* **2017**, *20*, 283-295; b) X. Chen, S. Shen, L. Guo, S. S. Mao, *Chem. Rev.* **2010**, *110*, 6503-6570; c) X. Wang, K. Maeda, A. Thomas, K. Takahashi, G. Xin, J. M. Carlsson, K. Domen, M. Antonietti, *Nat. Mater.* **2009**, *8*, 76-80.
- [2] a) A. V. Puga, *Coord. Chem. Rev.* **2016**, *315*, 1-66; b) M. F. Kuehnle, E. Reisner, *Angew. Chem. Int. Ed.* **2018**, *57*, 3290-3296.
- [3] V. Artero, M. Chavarot-Kerlidou, M. Fontecave, *Angew. Chem. Int. Ed.* **2011**, *50*, 7238-7266.
- [4] A. Mills, S. Le Hunte, *J. Photoch. Photobiol. A* **1997**, *108*, 1-35.
- [5] a) T. Kawai, T. Sakata, *Nature* **1980**, *286*, 474-476; b) A. Speltini, M. Sturini, D. Dondi, E. Annovazzi, F. Maraschi, V. Caratto, A. Profumo, A. Buttafava, *Photochem. Photobiol. Sci.* **2014**, *13*, 1410-1419; c) A. Caravaca, W. Jones, C. Hardacre, M. Bowker, *Proc. R. Soc. London, Ser. A* **2016**, *472*, 20160054.
- [6] X. Wu, X. Fan, S. Xie, J. Lin, J. Cheng, Q. Zhang, L. Chen, Y. Wang, *Nat. Catal.* **2018**, *1*, 772-780.
- [7] D. W. Wakerley, M. F. Kuehnle, K. L. Orchard, K. H. Ly, T. E. Rosser, E. Reisner, *Nat. Energy* **2017**, *2*, 17021.
- [8] a) H. Kasap, D. S. Achilleos, A. Huang, E. Reisner, *J. Am. Chem. Soc.* **2018**, *140*, 11604-11607; b) Q. Liu, L. Wei, Q. Xi, Y. Lei, F. Wang, *Chem. Eng.* **2020**, *383*, 123792; c) X. Xu, J. Zhang, S. Wang, Z. Yao, H. Wu, L. Shi, Y. Yin, S. Wang, H. Sun, *J. Colloid Interface Sci.* **2019**, *555*, 22-30.
- [9] D. S. Achilleos, H. Kasap, E. Reisner, *Green Chem.* **2020**, *22*, 2831-2839.
- [10] a) B. C. M. Martindale, G. A. M. Hutton, C. A. Caputo, E. Reisner, *J. Am. Chem. Soc.* **2015**, *137*, 6018-6025; b) B. C. M. Martindale, G. A. M. Hutton, C. A. Caputo, S. Prantl, R. Godin, J. R. Durrant, E. Reisner, *Angew. Chem. Int. Ed.* **2017**, *56*, 6459-6463.
- [11] G. A. M. Hutton, B. C. M. Martindale, E. Reisner, *Chem. Soc. Rev.* **2017**, *46*, 6111-6123.
- [12] M. A. Gross, A. Reynal, J. R. Durrant, E. Reisner, *J. Am. Chem. Soc.* **2014**, *136*, 356-366.
- [13] B. C. M. Martindale, E. Joliat, C. Bachmann, R. Alberto, E. Reisner, *Angew. Chem. Int. Ed.* **2016**, *55*, 9402-9406.
- [14] a) H. Kasap, C. A. Caputo, B. C. M. Martindale, R. Godin, V. W.-h. Lau, B. V. Lotsch, J. R. Durrant, E. Reisner, *J. Am. Chem. Soc.* **2016**, *138*, 9183-9192; b) H. Kasap, R. Godin, C. Jeay-Bizot, D. S. Achilleos, X. Fang, J. R. Durrant, E. Reisner, *ACS Catal.* **2018**, *8*, 6914-6926.
- [15] F. H. Isikgor, C. R. Becer, *Polym. Chem.* **2015**, *6*, 4497-4559.
- [16] a) B. C. Hodges, E. L. Cates, J.-H. Kim, *Nat. Nanotechnol.* **2018**, *13*, 642-650; b) A.-J. Simamora, F.-C. Chang, H. P. Wang, T.-C. Yang, Y.-L. Wei, W.-K. Lin, *Int. J. Photoenergy* **2013**, *2013*, 419182; c) L. Guo, Z. Yang, K. Marcus, Z. Li, B. Luo, L. Zhou, X. Wang, Y. Du, Y. Yang, *Energy Environ. Sci.* **2018**, *11*, 106-114; d) P. J. J. Alvarez, C. K. Chan, M. Elimelech, N. J. Halas, D. Villagrán, *Nat. Nanotechnol.* **2018**, *13*, 634-641; e) Y. Li, G. Lu, S. Li, *Appl. Catal. A* **2001**, *214*, 179-185; f) J. Kim, D. Monllor-Satoca, W. Choi, *Energy Environ. Sci.* **2012**, *5*, 7647-7656.
- [17] R. Godin, Y. Wang, M. A. Zwijnenburg, J. Tang, J. R. Durrant, *J. Am. Chem. Soc.* **2017**, *139*, 5216-5224.
- [18] a) J. Tang, J. R. Durrant, D. R. Klug, *J. Am. Chem. Soc.* **2008**, *130*, 13885-13891; b) S. Corby, L. Francàs, S. Selim, M. Sachs, C. Blackman, A. Kafizas, J. R. Durrant, *J. Am. Chem. Soc.* **2018**, *140*, 16168-16177; c) S. Selim, E. Pastor, M. García-Tecedor, M. R. Morris, L. Francàs, M. Sachs, B. Moss, S. Corby, C. A. Mesa, S. Gimenez, A. Kafizas, A. A. Bakulin, J. R. Durrant, *J. Am. Chem. Soc.* **2019**, *141*, 18791-18798.
- [19] A. Reynal, E. Pastor, M. A. Gross, S. Selim, E. Reisner, J. R. Durrant, *Chem. Sci.* **2015**, *6*, 4855-4859.
- [20] a) L. Sui, W. Jin, S. Li, D. Liu, Y. Jiang, A. Chen, H. Liu, Y. Shi, D. Ding, M. Jin, *Phys. Chem. Chem. Phys.* **2016**, *18*, 3838-3845; b) J. P. Guin, S. K. Guin, T. Debnath, H. N. Ghosh, *Carbon* **2016**, *109*, 517-528.

Entry for the Table of Contents



Biomass-derived materials photoconvert biomass: A triple natural resource system is reported that uses solar energy to convert biomass into sustainable H_2 and organics from untreated water. The process is photocatalyzed by scalable carbon dots produced from α -cellulose that act as a water-soluble light absorber to photoconvert lignocellulose with a Ni cocatalyst. The carbon dots are bestowed with suitable photophysical properties to function under ambient conditions and benign aqueous solution.